UNCLASSIFIED
SECURITY CLASSIFICATION OF THIS PAGE

REPORT DOCUMENTATION PAGE

1a. REPORT SECURITY CLASSIFICATION UNCLASSIFIED	1b. RESTRICTIVE MARKINGS
2a. SECURITY CLASSIFICATION AUTHORITY	3. DISTRIBUTION/AVAILABILITY OF REPORT Approved for public release; distribution is unlimited.
2b. DECLASSIFICATION/DOWNGRADING SCHEDULE	
4. PERFORMING ORGANIZATION REPORT NUMBER(S)	5. MONITORING ORGANIZATION REPORT NUMBER(S)
6a. NAME OF PERFORMING ORGANIZATION Naval Ocean Systems Center 6b. OFFICE SYMBOL (If applicable) NOSC	7a. NAME OF MONITORING ORGANIZATION
6c. ADDRESS (City, State and ZIP Code) San Diego, California 92152–5000	7b. ADDRESS (City, State and ZIP Code)
8a. NAME OF FUNDING/SPONSORING ORGANIZATION Office of Chief of Naval Research 8b. OFFICE SYMBOL (If applicable) OCNR	9. PROCUREMENT INSTRUMENT IDENTIFICATION NUMBER
8c. ADDRESS (City, State and ZIP Code) Independent Exploratory Development Programs (IED) OCNR-20T Arlington, VA 22217	10. SOURCE OF FUNDING NUMBERS PROGRAM ELEMENT NO. 0602936N PROJECT NO. ZE63 TASK NO. RV36I21 AGENCY ACCESSION NO. DN308 046

11. TITLE (Include Security Classification)

DRAG AND NOISE MEASUREMENTS ON AN UNDERWATER VEHICLE WITH A RIBLET SURFACE COATING

12. PERSONAL AUTHOR(S)

M. C. Gillcrist and L. W. Reidy

13a. TYPE OF REPORT	13b. TIME COVERED	14. DATE OF REPORT (Year, Month, Day)	15. PAGE COUNT
presentation/paper	FROM TO	September 1989	

16. SUPPLEMENTARY NOTATION

17. COSATI CODES			18. SUBJECT TERMS (Continue on reverse if necessary and identify by block number)
FIELD	GROUP	SUB-GROUP	skin drag boundary layer buoyant vehicle riblets

19. ABSTRACT (Continue on reverse if necessary and identify by block number)

From 50 to 80 percent of the energy expended by marine vehicles (ships, submarines, torpedoes, etc.) is used solely to overcome turbulent skin drag. It is not surprising, therefore, that both government and industry have invested heavily in research focused on the problem of turbulent skin friction. Of the many approaches to reduction of turbulent skin drag, the recently introduced riblet concept is among those that show the greatest promise for application to existing hull forms.

Published in *Drag Reduction In Fluid Flows*, editors R. H. J. Sellin, and R. T. Moses, 1989.

20. DISTRIBUTION/AVAILABILITY OF ABSTRACT	21. ABSTRACT SECURITY CLASSIFICATION
☒ UNCLASSIFIED/UNLIMITED ☐ SAME AS RPT ☐ DTIC USERS	UNCLASSIFIED

22a. NAME OF RESPONSIBLE INDIVIDUAL	22b. TELEPHONE (Include Area Code)	22c. OFFICE SYMBOL
M. C. Gillcrist	(619) 553–1602	Code 631

DD FORM 1473, 84 JAN

83 APR EDITION MAY BE USED UNTIL EXHAUSTED
ALL OTHER EDITIONS ARE OBSOLETE

UNCLASSIFIED
SECURITY CLASSIFICATION OF THIS PAGE

ELLIS HORWOOD PUBLISHERS

DRAG REDUCTION IN FLUID FLOWS

Techniques for friction control

editors R. H. J. Sellin and R. T. Moses

DRAG REDUCTION IN FLUID FLOWS

4.4 DRAG AND NOISE MEASUREMENTS ON AN UNDERWATER VEHICLE WITH A RIBLET SURFACE COATING

M.C. Gillcrist and L.W. Reidy – Naval Ocean Systems Center, San Diego, California.

INTRODUCTION

From 50 to 80 percent of the energy expended by marine vehicles (ships, submarines, torpedos, etc.) is used solely to overcome turbulent skin drag. It is not surprising, therefore, that both government and industry have invested heavily in research focused on the problem of turbulent skin friction. Of the many approaches to reduction of turbulent skin drag, the recently introduced riblet concept is among those that show the greatest promise for application to existing hull forms.

The use of streamwise microgrooves, or riblets, for turbulent skin friction reduction originated at NASA Langley for aerodynamic applications. The grooves are defined by peak height (h) and peak to peak spacing (s) as illustrated in Fig.1. For most practical drag reduction applications, the grooves are barely discernible to the naked eye. Although a wide range of groove geometries have been tested, researchers (references 1-3) have found that the sharply peaked symmetric v-groove ($h^+ = s^+ = 13$ to 15) is optimal, providing a decrease in skin friction of about 8%. The scaling parameter, s^+, is defined by equation 1.

$$s^+ = \frac{sU_\infty}{\nu}\sqrt{\frac{C_f}{2}} \qquad (1)$$

Recognizing the commercial potential of riblet technology, the 3M Company developed a technique to accurately manufacture riblets in an adhesive-backed extruded vinyl film. Encouraged by the effectiveness of riblets in the aerodynamic arena, hydrodynamicists have begun testing riblets in water. Experiments conducted in the Naval Ocean Systems Center (NOSC) water tunnel with riblets on a flat plate (references 3,4,5) have demonstrated hydrodynamic drag reductions which compare favorably with similar tests performed in

wind tunnels. Attempts to accurately measure the improved performance of riblet coated marine vehicles are rather limited. Drop tank tests conducted by the Naval Underwater Systems Center employing a 4 inch (0.102 m) diameter axisymmetric body (reference 6) indicate that riblets reduced skin friction by a maximum of 6.8%. The purpose of this study was to investigate both the drag and noise reducing effects of riblet surface coatings on full scale vehicles operating in the marine environment.

The turbulent boundary layer wall pressure fluctuations are generally proportional to the skin friction coefficient. For this reason, drag reduction techniques are good candidates for noise reduction investigation. An experiment, by Lancey of California State University at Fullerton and the authors of this report (reference 7), measured wall pressure fluctuations for 3M riblets on a flat plate in a wind tunnel. Pinhole measuring ports ($d^+ = 60$) allowed measurement of the majority of the turbulent boundary layer spectrum. A 2.8 dB reduction in unsteady wall pressure was measured at frequencies around the peak of the spectrum for riblet s^+ equal to 13. Encouraged by the favorable wind tunnel results, the authors felt that the effects of riblets on noise merited further investigation.

The primary objective of this research was to measure the change in drag and noise on a marine vehicle coated with riblets. In order to accomplish the stated objective, the riblets were tested on a large axisymmetric buoyant vehicle in a deep fresh water lake in northern Idaho. This report will outline the approach and present the results of this experiment.

BUOYANT TEST VEHICLE EXPERIMENT

Vehicle Description and Test Facility

The buoyant test vehicle (BTV), shown in Fig. 2, is owned and operated by the Admiralty Research Establishment, United Kingdom. The BTV is a torpedo shaped body, which, when hauled down to depth and then released, ascends back to the surface propelled solely by its buoyancy. Terminal velocity is quickly attained so that most of the ascent is at a constant speed. The terminal velocity can be varied from test to test by changing the net buoyant force with the addition or subtraction of lead ballast. Stabilizing fins ensure that the vehicle remains in the vertical plane during ascent. On board sensors monitor vehicle depth, pitch and yaw, from which the ascent speed and trajectory can be computed following a test series. The recorder section houses a tape recorder, power supply, control electronics and interface electronics to support a wide spectrum of sensors and instruments. The primary advantage of such a test vehicle is the absence of engine and propulsor noise, which makes it attractive for flow noise experiments. A secondary advantage lies in the fact that for a fixed net buoyancy, the terminal drag on the vehicle remains the same from test to test, thus, the efficacy of a drag reducing coating can be easily determined by measuring the difference in vehicle terminal velocity with and without the coating. The BTV, as configured for the riblet experiment, measured 295 inches (7.5 m) in length, 21 inches (0.53 m) in diameter, and could attain a speed of about 40 knots.

The test site, located in Bayview, Idaho on Lake Pend Oreille, is operated by the David Taylor Research Center's Acoustic Research Detachment. Lake Pend Oreille is well suited for experiments of this type because it has a low ambient noise level, is free from currents, has a uniform temperature profile below 150 ft (46 m) and is very deep. The lake's depth, over 1,200-ft (366 m), permits relatively long ascents at terminal velocity, thereby affording adequate time for data collection. The haul-down system, illustrated in Fig. 3, is driven by a shore based winch and is capable of hauling the test vehicle from the lake's surface to a depth of 1200-ft (366 m). If the lake above the vehicle is clear of recreational boat traffic, the BTV is released to "pop-up" to the surface.

Test Plan

The main purpose of this study was to assess the effect of riblets on both the noise and drag characteristics of marine vehicles, thus the primary goal of the BTV experiment was to measure vehicle speed and flow noise during the terminal velocity phase of the ascent. The test procedure called for data collection both with and without riblets. The only variable in the experiment, besides the presence or absence of riblets, was the vehicle net buoyancy, and this was varied by the addition of lead ballast. The weight and volume change due to the riblet coating alone altered the net buoyancy by approximately one pound, which translates into a 0.1% variation in terminal velocity. The lead ballast changes corresponded to three nominal speeds, henceforth referred to as high-speed, mid-speed and low-speed. The test plan called for a total of eighteen pop-ups (6 runs at each speed), half with riblets and half without riblets. The actual test program, yielded seventeen runs of useable data.

BTV Drag

The drag force, D, on a vehicle with cross sectional area, A, moving with velocity, V, can be computed as:

$$D = \frac{1}{2} C_d \rho A V^2 \tag{2}$$

where C_d, the nondimensional drag coefficient, is usually determined experimentally. The coefficient of drag can be thought of as a dimensionless value representing the distribution of pressure and shear-stress around the body. Thus one can think of C_d as consisting of one component which accounts for the form drag and another which accounts for the skin friction. Riblets can only reduce the shear-stress component of the drag and only on the coated portion of the vehicle's surface. Seventy-five percent of the total drag on the BTV is due to friction. Practicality dictated that only 76% of the BTV's surface be coated with riblets. If the riblet coated surface realizes a skin friction reduction of 8%, the overall drag reduction is calculated to be 5%. If we leave the vehicle's net buoyant force unchanged and run the vehicle with and without riblets, we would expect to measure two different terminal velocities, V' and V respectively, where $(V/V')^2 = C'_d/C_d$. For an overall drag reduction of 5%, $V' = 1.0236V$. This implies that the BTV will realize a 2.36% speed increase with the addition of riblets (covering 76% of the vehicle's surface), if the riblets provide the optimum skin friction reduction of 8%. This optimum value is predicted only if the riblets are correctly sized, that is , s^+ must fall between about 13 and 15. From equation 1 we see that s^+, at a given point on the vehicle, depends on the local skin friction coefficient, C_f, the free-stream velocity, U_∞, and the groove size, s. U_∞ equals the terminal velocity and is therefore the same for all points on the vehicle. Since C_f varies over the length of the BTV, the optimum riblet size, s, varies over the length as well. C_f along the uncoated BTV surface was predicted using a computer program which solves both the axisymmetric potential flow problem and the boundary layer equations. Knowing C_f, s^+ was then computed using equation 1. Fig. 4 presents a plot of s^+ versus position along the BTV for a vehicle speed of 39.7 knots and an s of 0.0013 inches (33 μm). It is clear from the figure, that for this speed and groove size, s^+ falls within the optimum range of 13 to 15 over most of the vehicle length. For this reason, the authors opted to apply only one riblet size, s = 0.0013 inches (33 μm), over the portion of the vehicle indicated.

BTV Speed

A pressure transducer mounted in the tail section was used to monitor the hydrostatic pressure the vehicle sees during its ascent to the surface. Following the test, the analog

signal was sampled to provide approximately 50 data points from the terminal velocity phase of the ascent. A linear fit of these data points was performed by ARE's computer program SPEEDFIT. Vehicle speed was obtained from the slope of this curve. The error in the curve fit velocity was less then 0.25% for all pop-ups.

The BTV test procedure involved performing pop-ups at a given net buoyancy both with and without riblets. Three nominal speeds were investigated: high speed, approximately 40 knots; mid-speed, approximately 34.5 knots; and low-speed, approximately 31.5 knots. A riblet size, s, was selected, as evidenced in the previous discussion of Fig.4, to produce an optimum s^+ at the BTV's top speed. It was believed that pop-ups at the mid and low-speed values would help establish the shape of the drag reduction versus velocity curve, in addition to providing flow noise data.

BTV Drag Results

Table 1 presents the speed and drag results of the seventeen pop-up tests conducted. A speed increase of 2.3% +/- .3% was measured for the vehicle ascending with riblets at the vehicle top speed. This compares favorably with the 2.36% speed increase predicted. The results of the mid and low-speed pop-ups appear to be somewhat inconsistent. The s^+ for the mid-speed runs ($12 < s^+ < 13$) should yield greater drag reduction than that for the low-speed tests ($11 < s^+ < 12$), however, the speed increases for both cases are practically identical (1.3% and 1.4% respectively).

Table 1. Buoyant Test Vehicle Speed and Drag Results

Test Case	Percent Speed Increase	Percent Skin Friction Reduction
High-Speed	2.3 +/- .3	7.7
Mid-Speed	1.3 +/- .3	4.4
Low-Speed	1.4 +/- .3	4.8

BTV Flow Noise Instrumentation

Four different types of noise data were obtained during the Buoyant Test Vehicle pop-ups:

1) turbulent boundary-layer pressure fluctuation data from individual flush-mounted piezoelectric pressure transducers along the side of the vehicle;
2) accelerometer data;
3) self-noise data from the nose sonar array; and
4) self-noise data from a flank array.

Results from the flush-mounted individual pressure transducers and accelerometers are reported in this paper. The self-noise data from the nose array was collected and analyzed by the Naval Underwater Systems Center (T. Galib), and shows that within the uncertainty of these measurements, there was no difference between the baseline runs and the riblet runs. The flank array data was collected and analyzed by the British Admiralty Research Establishment (J. Bainbridge), and shows an increase in noise due to riblets of up to 10 dB for the acoustic field between 30 kHz and 135 kHz. This unexpected result is still under investigation and will not be discussed here.

The output from two accelerometers and four individual flush-mounted pressure transducers was recorded on board the vehicle. Figure 2 shows the locations of the transducers that were used, referred to in this report as PT1, PT2, PT3, and PT4. PT1 and PT2 were PCB model 105A03 sensors with 0.1 inch (0.25 cm) diameter faces, while PT3 and PT4

were PCB model 112A21 sensors with 0.218 inch (0.55 cm) diameter faces. Both models were quartz piezoelectric transducers with stainless steel casings. The accelerometers were PCB model 303A02, mounted on the inside surface of the vehicle shells. Accelerometer 1 was in the immediate vicinity of PT1 and PT2, and accelerometer 2 was in the immediate vicinity of PT3 and PT4. This data was recorded with the on board Honeywell 5600 tape recorder using wide band FM channels at a tape speed of 60 inches per second (1.5 m/s). Following a series of pop-ups, a strip chart recorder was used to reproduce the data in hard copy form. The noise data was analyzed on-site using a Hewlett Packard 3561A spectrum analyzer, a . an rms averaging circuit.

Since the effect of the application of vinyl coatings over the faces of the flush-mounted transducers is not well understood, tests were conducted in a water tank prior to the BTV tests in Idaho. Two methods were determined to be valid for comparing baseline and riblet buoyant vehicle runs. Both methods involved coating the vehicle surface in the vicinity of the transducers with plain smooth vinyl film, 0.003-inch (76 μm) thick, for the baseline runs and with v-groove film (0.003-inch thick plus the grooves) for the riblet runs. In addition, both methods required slicing the film coating around the circumference of the transducer faces. The difference between the two methods is simply that in method-1 the circular patch of film on the transducer face is removed, while in method-2 the film on the transducer face is allowed to remain. Method-2 was employed for transducers PT2 and PT4, and method-1 was used for transducer PT1. Neither method was applied to transducer PT3. The film covering PT3 was not cut.

BTV Flow Noise Results

The level of rms wall pressure fluctuations increases approximately with the square of velocity. Because the riblet coating results in a measured gain in vehicle speed, the expected rise in sound pressure level can be computed. This increase in sound pressure level is predicted to be 0.39 dB for the high-speed test configuration. However, the data from the flush-mounted pressure transducers shows essentially no difference between baseline and riblet runs. This indicates that the additional speed due to the presence of the riblets was achieved without the rise in noise level that usually accompanies an increase in velocity.

A typical pressure transducer spectrum from PT4 is shown in Figure 5, comparing one of the high speed baseline runs to one of the high speed riblet runs. The levels are reported as dBV, which is voltage output from the transducers and amplifier cards relative to 1 Volt. The ambient levels were recorded prior to the release of the vehicle as a check. On a spectrum of this type, it is not possible to distinguish 0.39dB in comparing the baseline and riblet runs. Comparisons of PT4 and Accelerometer 2 show different frequency content below 10kHz, indicating that for those frequencies the predominant pressure transducer response is not due to shell vibrations. Below approximately 7.5 kHz, the pressure transducer is believed to be responding to the wall pressure fluctuations impinging on the transducer. Between 7.5kHz and 40kHz, it is probably responding to a combination of the radiated acoustic flow noise and shell vibrations, and above 40kHz, the FM recording is not usable.

The rms average for PT4 is plotted versus vehicle speed in Figure 6. Each point is the average of three runs (two runs for the low speed baseline). The average standard deviation of the rms averages for the baseline runs was 0.23dBV. The uncertainty based on the divisions used for reading values off the strip chart, however, is ±0.5dBV. When the data for PT1, PT2, PT3 and PT4 are all examined, it appears that the speed advantage of the riblets was gained without an associated increase in noise. This is especially true for the

transducers that had riblet material on their measuring faces, PT2 and PT4. It should be noted, however, that because the transducer diameters were large compared to the boundary layer thickness ($d^+ > 890$), the wall pressure fluctuations were only measured for the low frequency end of the turbulent boundary layer spectrum.

CONCLUSIONS

Experiments were conducted to determine the effects of riblet coatings on the drag and noise characteristics of an underwater vehicle. The v-groove vinyl riblet coating, made by the 3M Company, was applied to the majority of the turbulent boundary layer region of an axisymmetric buoyant body. A velocity increase of 2.3% +/-0.3% was measured. This velocity increase was in agreement with predictions based on 8% skin friction reduction for the area covered with the riblet material. Pressure transducers mounted on the side of the vehicle indicated that the low frequency turbulent boundary layer noise did not increase due to the increase in speed caused by the riblets.

ACKNOWLEDGEMENTS

We would like to thank the 3M Company for providing the riblets used in this research. We are also grateful to our colleagues at Admiralty Research Establishment, Naval Underwater Systems Center and David Taylor Research Center for their invaluable help and technical support. This work was accomplished under the Independent Research/Independent Exploratory Development Program at Naval Ocean Systems Center.

REFERENCES

1. Walsh, M. J., "Riblets as a Drag Reduction Technique," AIAA Journal, Volume 21, No. 4, April 1983.

2. Wilkinson, S. P., Anders, J. B., Lazos, B. S., and D. M. Bushnell, "Turbulent Drag Reduction Research at NASA Langley: Progress and Plans," International Journal of Heat and Fluid Flow, Volume 9, No. 3, Sept. 1988.

3. Reidy, L. W., "Flat Plate Drag Reduction in a Water Tunnel Using Riblets," Naval Ocean Systems Center Technical Report 1169, May 1987.

4. Reidy, L. W., and G. W. Anderson, "Drag Reduction for External and Internal Boundary Layers Using Riblets and Polymers," AIAA-88-0138, AIAA 26th Aerospace Sciences Meeting, Reno, Nevada, Jan. 11-14, 1988.

5. Reidy, L. W., "Flat Plate Drag Reduction in a Water Tunnel Using Riblets," Proceedings of the 17th AIAA Symposium on the Aero/Hydronautics of Sailing, Volume 34, Stanford, California, Oct. 31 - Nov. 1, 1987.

6. Beauchamp, C. H., and R. B. Philips, "Riblet and Polymer Drag Reduction on an Axisymmetric Body," Symposium on Hydrodynamic Performance Enhancement for Marine Applications, sponsored by the Naval Underwater Systems Center and the University of Rhode Island, Newport, Rhode Island, Oct. 31 - Nov 1, 1988.

7. Lancey, T. W., and L. W. Reidy, "Effects of Surface Riblets on the Reduction of Wall Pressure Fluctuations in Turbulent Boundary Layers," Research Brief, Journal of the Acoustical Society of America, April 1989.

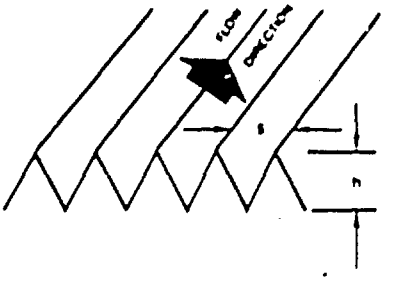

Figure 1. Riblet Groove Geometry (h=s)

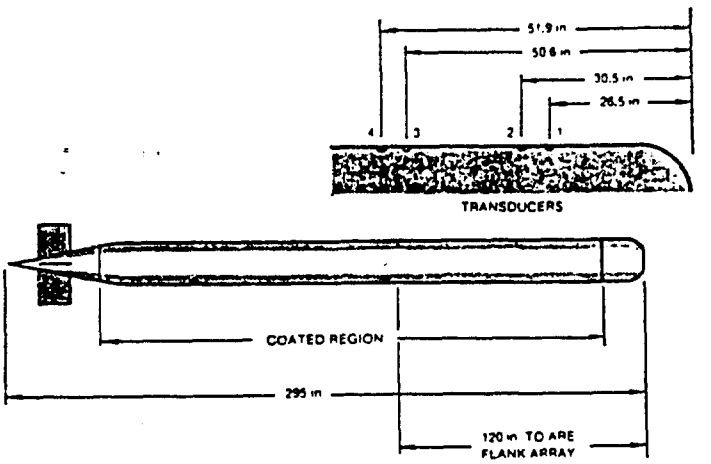

Figure 2. Schematic Drawing of the Buoyant Test Vehicle

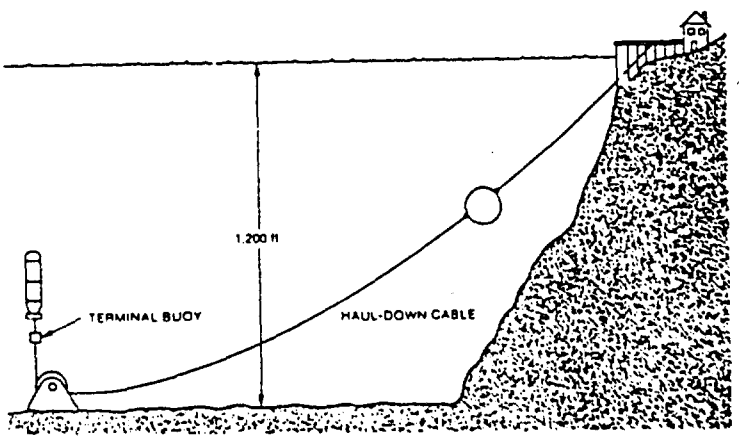

Figure 3. Schematic Drawing of the Buoyant Test Vehicle Haul-down System

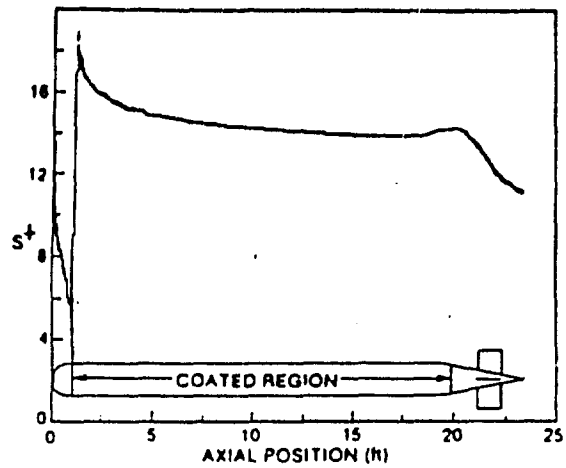

Figure 4. s^+ vs. BTV Length for s=0.0013inch Riblets at High Speed

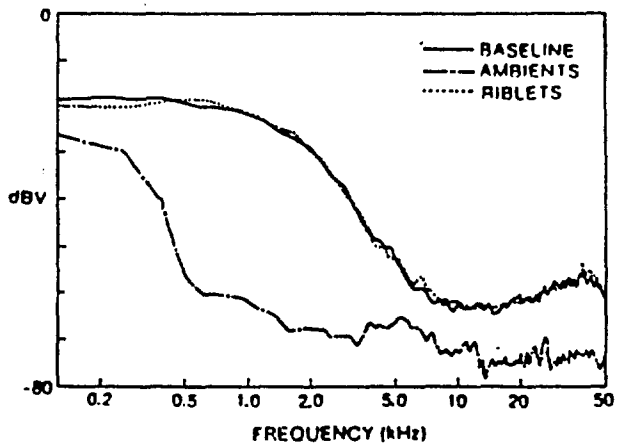

Figure 5. Frequency Spectra for BTV Pressure Transducer 4 during High Speed Runs

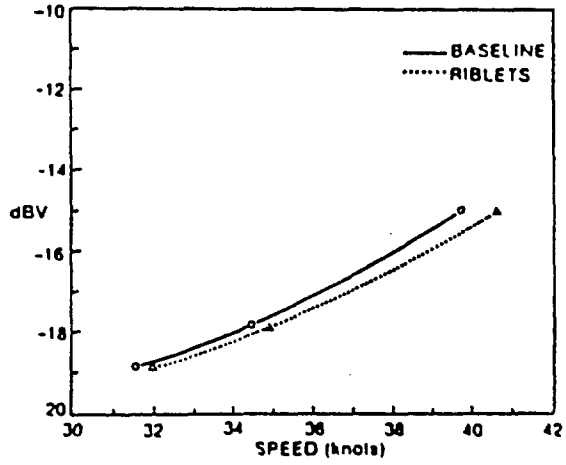

Figure 6. RMS Average for BTV Pressure Transducer 4 in dBV vs. Vehicle Speed